Synthesis and Characterization of Spiro-Triphenylamine Configured Polyfluorene Derivatives with Improved Hole Injection

Doojin Vak,[†] Jang Jo,[†] Jieun Ghim,[†] Chaemin Chun,[†] Bogyu Lim,[†] Alan J. Heeger,[†,‡] and Dong-Yu Kim*[,†]

Heeger Center for Advanced Materials, Gwangju Institute of Science and Technology, 1 Oryong-dong, Buk-gu, Gwangju, Korea, and Physics Department and Materials Department, University of California, Santa Barbara, California 93106

Received March 26, 2006; Revised Manuscript Received July 13, 2006

ABSTRACT: We report on the synthesis of a spiro-fluorene derivative with bulky *tert*-butyl-substituted triphenylamine structure. The compound was synthesized in an attempt to enhance both hole injection and physical properties. A series of copolymers of the compound and a spiro-anthracenefluorene structure were synthesized, and their physical, optical, and electrochemical characteristics were investigated. The polymers showed good thermal stability with decomposition temperatures in excess of 389 °C and high glass transition temperatures in the range of 112−207 °C. The emission characteristics of the polymers were similar to that of dialkyl polyfluorenes. Cyclic voltametry studies revealed that the energy level of polymers can be tuned by adjusting the spiro-triphenylamine content with a tuning range of about 0.5 eV. Organic light-emitting diodes were fabricated using the polymers. All of the devices showed an emission in the deep blue region, and the copolymers showed improved hole injecting/transporting characteristics.

Conjugated polymers have attracted considerable research interest in the past decade due to their potential applications in the areas of large area plat panel display and other optoelectronic devices.[1,2] Organic light-emitting diodes (OLEDs) are promising devices for use in full color plat panel displays and have a number of advantages over conventional devices such as a low driving voltage, wide viewing angle, thin film structure, and a simpler manufacturing process.[3] Polymer-based OLEDs have a considerable potential for use in flexible displays.[4] Various conjugated polymers have been developed for such applications. Among them, polyfluorene derivatives (PFs) have generated considerable interest as blue-emitting materials due to their high photoluminescence (PL) efficiency, wide band gap for blue emission, and thermal stability.[5−9] In addition, the ability to readily functionalize the C-9 position of the fluorene unit is one of the advantages of these types of compounds. Various solublizing alkyl chains or side groups have been introduced at this position. However, the C-9 position of the fluorene unit recently has been regarded as a problem. List et al. reported that the degradation of blue emission of PFs was due to oxidation of the C-9 position to form fluorenone, the emission of which is similar to the broad band emission of degraded PFs, in conjugated backbones the so-called keto defect.[10] Keto defects can be formed not only by photoirradiation or heat treatment but during the operation of device via electrooxidation. The appearance of a broad band emission of PFs in the green region, the so-called g-band, constitutes an important issue in terms of enhancing OLED lifetime and has been attributed to a physical defect, aggregate formation followed by excimer emission.[11−15] The results of more recent studies suggest that this can be attributed to chemical degradation.[16−19] Although keto defects are currently believed to be the most probable source of long wavelength emission, the chemical defect model does not completely explain some phenomena such as the enhanced stability by cross-linking,[20,21] copolymerization with bulky groups,[22] blending,[23] introduction of complex backbone structures,[24] the dependency on the length of alkyl groups,[25] and the increase in long wavelength emission in the solution state by enhanced molecular interaction.[26] Therefore, both models are needed to completely explain all of the experimental observations. Although the major reason for the appearance of g-bands is still not clear, most previous reports have concluded that the introduction of bulky phenyl side groups instead of long alkyl chains can effectively suppress the degradation phenomenon.[27−35] The reason for this is that bulky phenyl side groups not only enhance physical properties in a fully amorphous state and enhance glass transition temperature of polymers followed by reduced aggregate formation but also enhance the chemical stability toward oxidative degradation due to the more stable $C(sp^2)-C(sp^2)$ bonds at the C-9 position of fluorene units compared to the $C(sp^2)-C(sp^3)$ bonds of conventional alkyl-substituted PFs.

One of the useful bulky phenyl side groups is a fluorene unit itself connected by a spiro-linkage, referred to as a spiro-bifluorene. A spiro-bifluorene contains two biphenyl units connected by a tetrahedrally bonded carbon atom, in which the planes of the biphenyl units lie perpendicular to each other. Once incorporated into PFs, this three-dimensional structure should prevent the approach of other polymer backbones, and therefore aggregate formation of the conjugated polymer backbone would be minimized efficiently. Although the introduction of a spiro-bifluorene into PF has been shown to alleviate the spectral stability problem,[32] its incorporation into the polymer structure greatly reduces its solubility in common organic solvents. As a result, no homopolymer of spiro-bifluorene has been reported. We recently reported on poly[10,10-bis(2-ethylhexyl)-10*H*-spiro(anthracene-9,9′-fluorene)-2′,7′-diyl] (PEHSAF), which contains a spiro-anthracenefluorene (SAF) rather than a spiro-bifluorene.[33] The SAF structure still contains the useful spiro-structure and, at the same time, permits the facile functional-

[†] Gwangju Institute of Science and Technology.
[‡] University of California, Santa Barbara.
* Corresponding author: Tel +82-62-970-2319, Fax +82-62-970-2304, e-mail kimdy@gist.ac.kr.

10.1021/ma060683o CCC: $33.50
Published on Web 08/19/2006

Chart 1

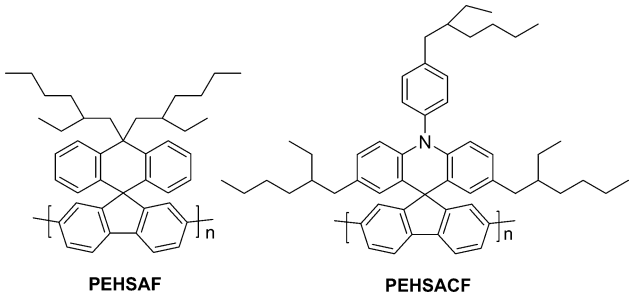

ization of the C-10 position of the dihydroanthracene unit. The polymer not only showed stable photoluminescence (PL) spectra after thermal treatment and photoirradiation but also showed excellent characteristics as an organic laser material due to its stable amorphous state. Bradley's group reported that the polymer showed an amplified spontaneous emission up to 250 °C (limited by the apparatus) with very low optical loss (loss coefficient = 0.8 cm^{-1}) and PL efficiency higher than PFs.[36]

Although PEHSAF showed enhanced physical properties, it still has the intrinsic problem associated with PFs. Since low work function metals are preferred as the anode in PFs-based OLEDs, imbalanced carrier injection continues to be a problem because the ionization potential of PFs is −5.8 eV[37] and that of poly(ethylenedioxythiophene):poly(styrenesulfonate) (PEDOT:PSS) is −5.2 eV.[38] This indicates that a significant energy barrier for hole injection exists, while the energy barrier for electron injection is very small when calcium, which is one of the most frequently used metals in large band-gap materials, is used as a cathode. Several studies have reported improvements in hole injecting and transporting properties when a phenylamine structure is introduced into conjugated polymers as an end-capper or as a side group.[39−41] These reports showed that the introduction of structures containing a heteroatom is a useful route for producing an efficient device. We recently reported on poly[10-(4-(2-ethylhexyl)-phenyl)-2,7-bis(2-ethylhexyl)-10*H*-spiro(ancridine-9,9′-fluorene)-2′,7′-diyl] (PEHSACF).[42] PEHSACF contains spiro-triphenylamine (TPA) structure with ethylhexyl solubilizing chains. Although the polymer adopted both a physically stable spiro-structure and an electronically preferred phenylamine structure, the structure contains a chemically unstable benzylic position which is susceptible to oxidation.

In this article, we report on a new spiro-fluorene unit containing spiro-TPA structure with chemically stable *tert*-butyl groups and its polymers. A series of copolymers based on this structure and hexadecyl-substituted SAF structure were synthesized with various feed ratios. The thermal, optical, and electrochemical properties of the polymers were investigated, and OLEDs based on the polymers were fabricated and characterized.

Results and Discussion

Synthesis and Characterization of Polymers. The synthesis of monomers is shown in Scheme 1. The bulky *tert*-butyl-substituted triphenylamine was synthesized via a Friedel−Crafts alkylation reaction. The solvent, trifluoroacetic acid, was used for activation of *tert*-butyl alcohol. Because of the reduced solubility of the alkylated TPA in the solvent compared to nonsubstituted TPA, the product precipitated during the reaction. Therefore, not only the reaction temperature but also the amount of solvent used found to be was very important. After optimizing the reaction conditions, **1** was easily obtained in high purity by a by simple filtration process. **2** was synthesized via the well-known highly selective bromination method.[43] Although DMF is typically used for the bromination reaction, we used dichloromethane as a cosolvent due to the low solubility of **1** in DMF. To **1** in dichloromethane solution, *N*-bromosuccinimide in DMF solution was slowly added dropwise at room temperature.

Scheme 1. Synthesis of Monomers

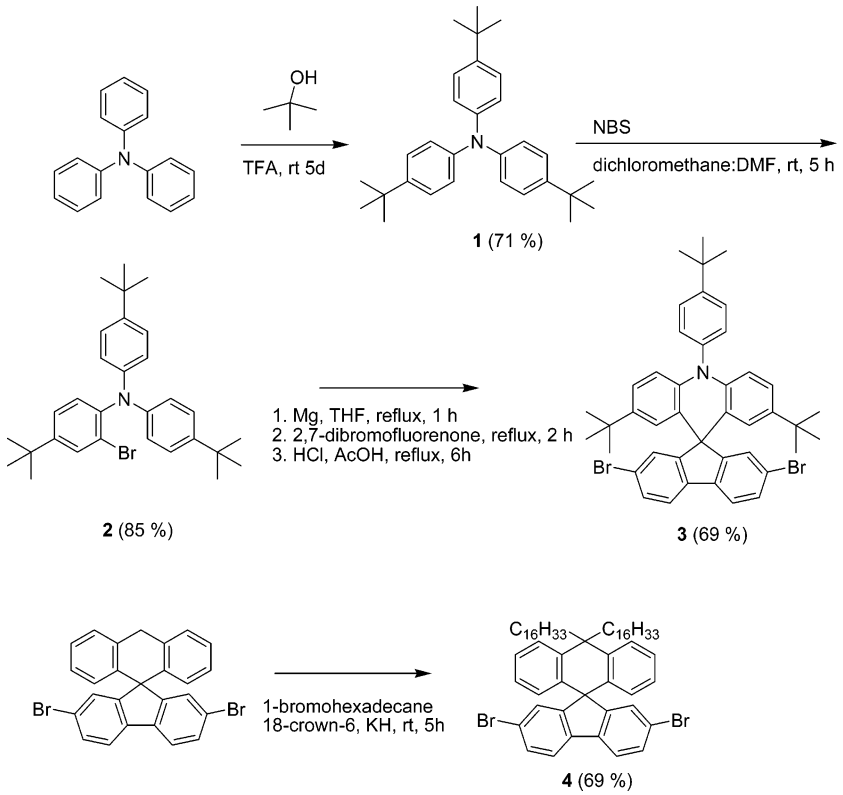

Scheme 2. Polymerization of PSAF16 and PSAF Copolymers with Different Feed Ratios

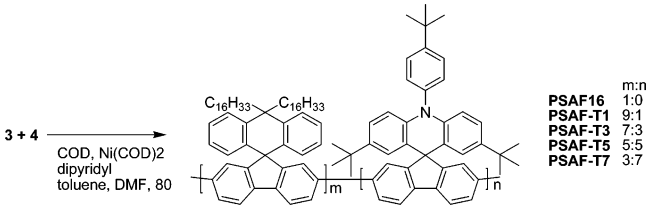

Table 1. Molecular Weights, Glass Transition Temperature, and Decomposition Temperatures of the Polymers

polymer	M_n[a] (g/mol)	M_w[a] (g/mol)	PDI[a]	T_g[b] (°C)	T_d[c] (°C)
PSAF-T7	23 000	68 000	2.95	207	404
PSAF-T5	17 000	44 000	2.58	165	396
PSAF-T3	15 000	38 000	2.53	130	392
PSAF-T1	11 000	27 000	2.45	112	385
PSAF16	11 000	24 000	2.18	145	389

[a] Molecular weights and polydispersity index (PDI) were estimated by GPC against polystyrene standards. [b] Glass transition temperature measured by DSC under nitrogen. [c] Temperature resulting in a 5% weight loss based on the initial weight.

Careful GC/MS analysis showed that a trace of dibromination was occurred during the reaction. The addition of a solution of **2** in THF to flame-dried Mg, followed by refluxing for 1 h produced the Grignard reagent of **2**. The Grignard reagent was added by 2,7-dibromofluorenone and refluxed for 2 h to produce an intermediate of spiro-structure. The intermediate contained a *tert*-alcohol at C-9 position of the fluorene unit. The C-9 position of fluorene unit was activated under acidic conditions and reacted with the TPA part via intramolecular cyclization to form **3**. **4** was synthesized using nearly the same way for the synthesis of an ethylhexyl-substituted SAF structure.[33] An anion was produced by the elimination of proton at the C-10 position of dihydroanthracene structure by treatment with the strong base KH, and the resulting anion was reacted with 1-bromoexadecane in situ.

A series of copolymers of **3** and **4** were synthesized via nickel-mediated polymerization using various feed ratios. The scheme for the polymerization is shown in Scheme 2. We attempted to synthesize a homopolymer of **3**. However, because of the low solubility of the unit, the polymer precipitated during the polymerization reaction, resulting in polymer with a very low molecular weight. We reported on the poly(spiro-anthracenefluorene) (PSAF) homopolymer with ethylhexyl side chains, PEHSAF.[33] The polymer was sufficiently soluble to permit solution processing. However, the ethylhexyl group was not effective as a solublizing group for the copolymer of PSAF and **4**. Therefore, a hexadecyl group was introduced into the SAF structure. All copolymers showed molecular weights higher than tens of thousands and showed good solubility in common organic solvents such as chloroform, toluene, and chlorobenzene. The characteristics of the copolymers are summarized in Table 1.

Figure 1 shows TGA and DSC curves for the polymers. The polymers showed decomposition temperatures (T_d, 5 wt % loss) from 385 to 404 °C. These high decomposition temperatures indicate that the introduction of anthracene or TPA as spiro-structures does not reduce the thermal stability of the polymers. Moreover, polymers with higher TPA contents showed a higher main decomposition temperature than that of polymers with lower TPA contents. The polymers with high TPA contents not only showed higher T_d values but also higher glass transition temperatures (T_g), except the homopolymer PSAF16. We attribute this phenomenon to the reduced crystallinity of linear long alkyl chains of the homopolymer. Addition of small portion of comonomer can disturb the crystallization of side chains. Although DSC curves of PSAF-T7 and PSAF16 are not clear to determine T_g, their transition ranges are higher than that of conventional dialkyl-substituted PFs. The T_g for dihexyl-substituted PF (PF6) is known to be about 100 °C. Because light-emitting polymers in OLED are degraded by the Joul heat generated during device operation, a high T_g is an the absolute requirement for polymers intended for use in OLED applications.

Table 2. Absorption and Emission Properties, Absolute Photoluminescence Quantum Efficiencies and HOMO and LUMO Energy Levels of the Polymers

polymer	abs λ_{max} (nm)	PL λ_{max} (nm)	Φ_{PL}[a] (%)	E_g[b] (eV)	HOMO[c] (eV)	LUMO[d] (eV)
PSAF-T7	400	422	26	3.0	−5.36	−2.36
PSAF-T5	400	422	36	3.0	−5.65	−2.65
PSAF-T3	402	423	47	3.0	−5.69	−2.69
PSAF-T1	402	437	69	3.0	−5.73	−2.73
PSAF16	402	438	59	3.0	−5.84	−2.84

[a] PL quantum efficiencies in film measured in an integrating sphere. [b] Optical band gap calculated from absorption spectra edge. [c] Determined by extrapolation of oxidative CV curves. [d] LUMO = HOMO + E_g.

Table 3. Characteristics of OLEDs with the Configuration of ITO/PEDOT:PSS (40 nm)/Emitting Polymer (70 nm)/LiF (5 nm)/Ca (30 nm)/Silver (200 nm)

polymer	luminance (cd/m^2)	QE (%)	turn-on[a] (V)	LE (cd/A)	PE (m/W)	CIE (x, y)
PSAF-T7	1298	0.07	5.9	0.11	0.07	0.196, 0.186
PSAF-T5	1383	0.13	5.4	0.19	0.07	0.191, 0.182
PSAF-T3	1160	0.19	6.1	0.25	0.09	0.184, 0.169
PSAF-T1	912	0.21	5.1	0.28	0.12	0.176, 0.150
PSAF16	574	0.13	6.2	0.19	0.07	0.183, 0.178

[a] Turn-on voltage, determined as the voltage required to give a luminance of 1 cd/m^2.

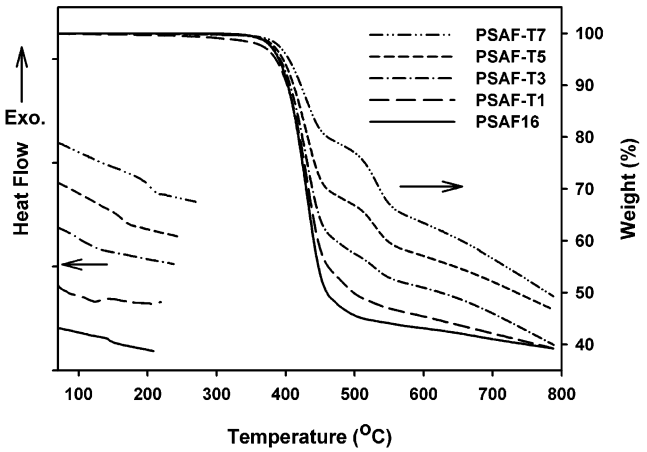

Figure 1. TGA and DSC curves for PSAF16 and copolymers.

Optical Properties of Polymers. UV/vis absorption and photoluminescence spectra are shown in Figure 2. All PSAF copolymers showed nearly the same absorption maxima at 400 nm, and exactly the same absorption onset at 413 nm where the corresponding optical band gap was 3.0 eV. The PL spectra of PSAF-T7, PSAF-T5, and PSAF-T3 showed emission peaks similar to PF6. However, the PL spectra for PSAF-T1 and PSAF16 were quite different. Since PEHSAF, a SAF homopolymer with ethylhexyl side chains, showed nearly the same emission peak positions, the red shift can be attributed to the long alkyl chains of the polymer. PSAF16 contains so long alkyl

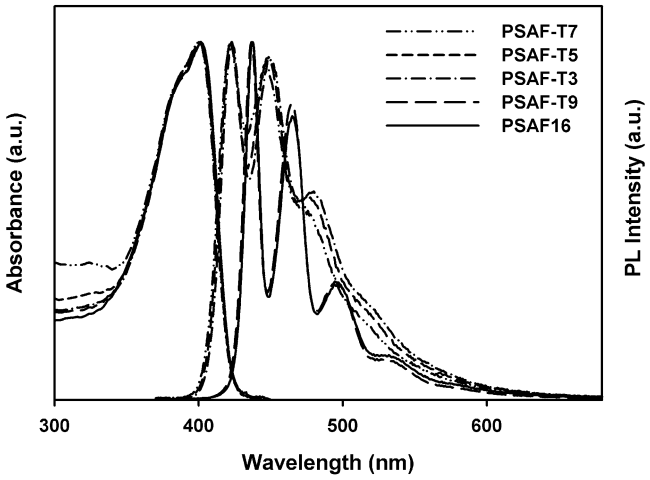

Figure 2. Absorption spectra in solution and PL spectra in polymer films.

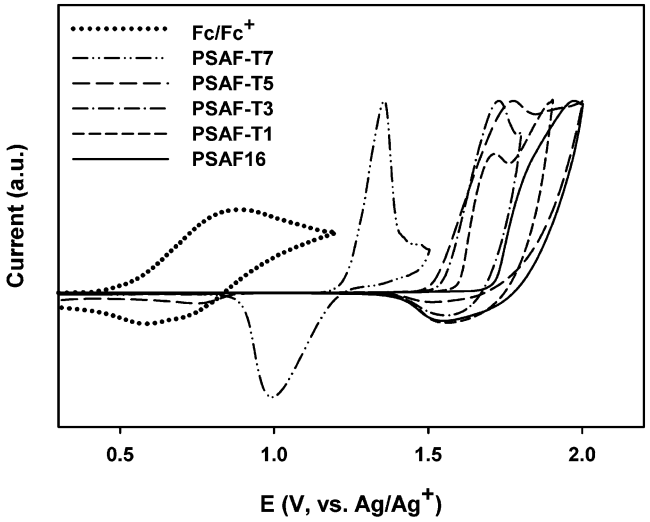

Figure 3. Cyclic voltamograms of polymers and ferrocene used as a reference. Measurements were carried out in 0.1 M Bu_4NClO_4 in acetonitrile solution with a scanning rate of 50 mV/s.

chains and such structures are known to induce a greater order of polymer chains in the solid state and can change the dihedral angle of the fluorene units. This phenomenon has also been observed in PFs.[44]

We measured the PLQE of polymer film on quartz plate in an integrating sphere following the literature procedure[45] and calculated the values relative to a known material, PEHSAF.[35] Since a thick film with an absorbance higher than 1.0 is recommended[46] and there was considerable thickness dependence on PLQE in our experiment when thin films with absorbance of less than 1.0 were used, we measured PLQE of samples with an absorbance of 1.0 or higher than 1.0. The PLQEs were reproducible with about a ±5% error range. Since a SAF polymer, PEHSAF, showed a higher PLQE than conventional PFs, PSAF16 and PSAF-T1 showed very high PLQE values. However, polymers with high TPA contents showed a reduced PLQE.

The energy levels of the PSAF copolymers were characterized by CV. CV curves of polymers and ferrocene are shown in Figure 3. The half-wave potential of ferrocene/ferrocenium (Fc/Fc^+) is known to be 4.8 eV below the vacuum level[47] and was used as a calibration reference. Although the optical band-gaps of PSAF copolymers were similar, there were significant differences in the highest occupied molecular orbital (HOMO) energy levels of polymers. The polymer with the highest TPA content, PSAF-T7, showed an HOMO energy level at −5.36 eV, which is nearly the same as the spiro-TPA homopolymer, PEHSACF. The HOMO energy levels of the polymers increased with decreasing TPA content. The differences between HOMO energy levels of PSAF-T5, PSAF-T3, and PSAF-T1 were very small, but there was significant difference between these of PSAF-T7 and PSAF-T5. The results were reproducible, and we conclude that there was no linear relationship between amount of TPA structure and HOMO energy level. The SAF homopolymer, PSAF16, showed nearly the same HOMO energy level as that of PF6. From these results, we expected enhanced hole injection in PSAF copolymers.

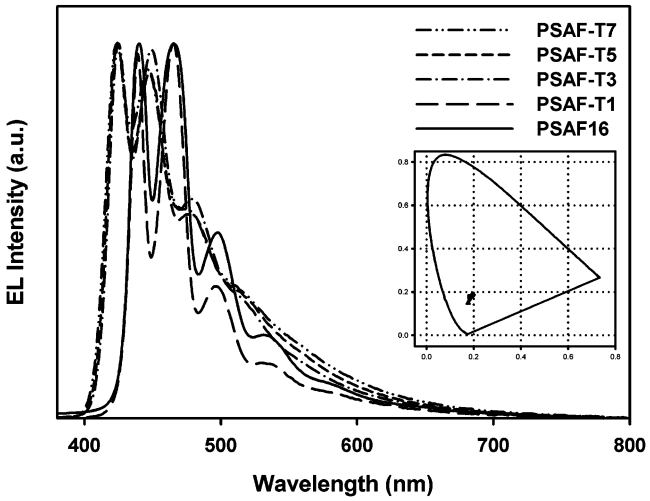

Figure 4. EL spectra of PLED with the configuration of ITO/PEDOT:PSS (40 nm)/emitting polymer (70 nm)/LiF (5 nm)/Ca (30 nm)/silver (200 nm). Inset shows CIE 1931 color coordinates of the EL spectra.

Device Characteristics. OLEDs with PSAF16 and its copolymers were fabricated with the configuration of ITO/PEDOT:PSS/emitting polymer/LiF/Ca/Ag. The LiF/Ca structure was adopted as a cathode because it is one of the most efficient electron injecting cathodes,[48] and silver was used as a protecting layer. Electroluminescence (EL) spectra of devices are shown in Figure 4. The EL spectra of polymers are nearly the same as the PL of the polymers. Although there were considerable differences in EL spectra, all EL spectra were still in the deep blue region with Commission Internationale de I′Eclairage (CIE) 1931 color coordinates of less than 0.2 for both *x* and *y*. The inset in Figure 3 shows the CIE color coordinates of the polymers.

Some representative current density−voltage (*J*−*V*) and luminance−voltage (*L*−*V*) curves are shown in parts a and b of Figure 5, respectively. Figure 5a clearly shows the effect of TPA structure. PSAF copolymers with higher TPA contents showed higher current density. However, PSAF16 showed a higher current density than PSAF-T1 and PSAF-T3 in the low current density regions. This is due to the low injection barrier of electrons as shown in Figure 6. However, the current densities of the copolymers became higher than that of PSAF16 at high injection level due to low mobility of electron. Because the emission of an OLED depends on both holes and electrons, the luminance characteristics are not linearly dependent on the TPA content. However, all copolymer showed better luminescence characteristics than that of PSAF16 due to the efficient hole injection and transport properties. Although, copolymers with higher TPA contents showed a higher current density and luminescence, the copolymers showed a reverse relationship between TPA content and external quantum efficiencies. As

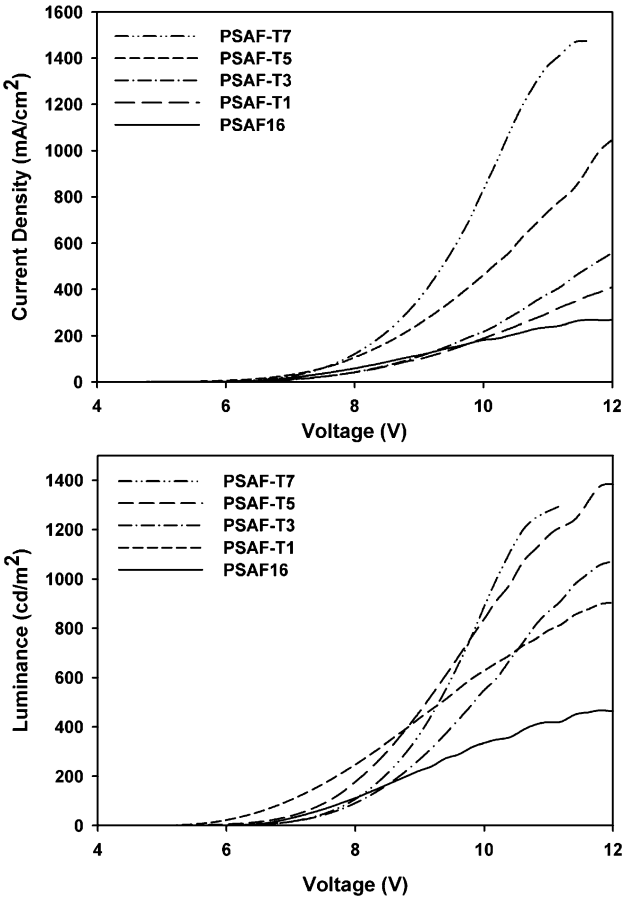

Figure 5. (a) Current density−voltage and (b) luminance−voltage curves of PLED with the configuration of ITO/PEDOT:PSS (40 nm)/emitting polymer (70 nm)/LiF (5 nm)/Ca (30 nm)/silver (200 nm).

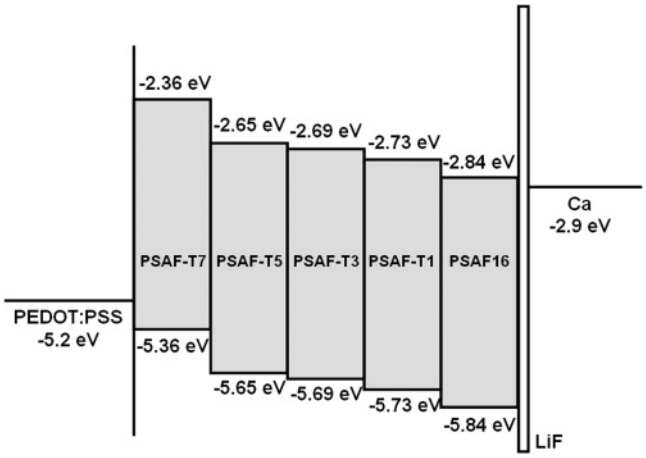

Figure 6. Schematic energy levels for electrodes and polymers.

shown in Figure 6, the HOMO energy level of PSAF-T7 was modified excessively. Therefore, the polymer showed the highest current density, much of which would be wasted as a leakage current. The phenomenon decreased with decreasing TPA content, and PSAF-T1 showed the highest external quantum efficiency. However, these results are not reasonable when both energy barriers are considered for electron and hole injection. PSAF-T1 has energy barriers of 0.17 eV for an electron and 0.53 eV for a hole, and the energy barriers of PSAF-T5 and PSAF-T3 are more balanced energy barriers than PSAF-T1. This problem can be solved by considering the PLQE of the polymers. The external quantum efficiency is linearly related

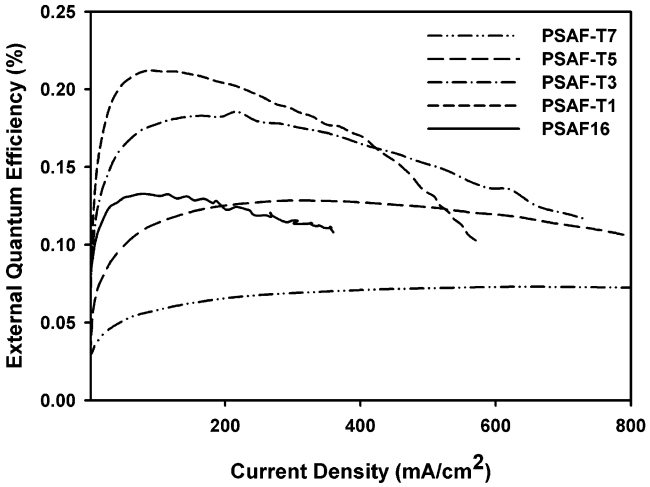

Figure 7. External quantum efficiency−current density curves of PLEDs with the configuration of ITO/PEDOT:PSS (40 nm)/emitting polymers (70 nm)/LiF (5 nm)/Ca (30 nm)/silver (200 nm).

to the ratio of the number of exciton formation events within the device to the number of electrons flowing in the external circuit and the efficiency of the radiative decay of excitons.[2] The former is the same as the carrier balance factor, and the latter is the same as PLQE. Therefore, the external quantum efficiencies divided by the PLQE value should be used to consider charge carrier balances. Using this concept, we conclude that the introduction of a spiro-TPA structure can enhance device performance with respect to carrier injection, transport, and balance, the carrier balance is optimized at the 30% TPA content, PSAF-T3, and an excess of TPA structure can degrade the device performance.

Summary

We synthesized spiro-PF copolymers with various contents of spiro-TPA. All polymers showed good optical properties as blue-emitting materials and enhanced thermal properties with higher T_g values than conventional PFs. The energy levels of the polymers were controlled by the amount of spiro-TPA content from −5.36 to −5.84 for HOMO and from −2.36 to −2.84 for LUMO. A copolymer with the highest spiro-TPA content showed the highest current density when the OLED device was fabricated, and the amount of spiro-TPA content was optimized in 30% with respect to charge carrier balance. This study will be useful in molecular engineering of polymers for OLED, and the spiro-TPA structure will be useful as a comonomer to modify the energy levels of PF derivatives without degradation in physical and electrooptical properties.

Experimental Section

Characterization and Measurements. Materials were characterized by means of ^{1}H and ^{13}C NMR spectroscopy (JEOL JNM-LA300WB 300 MHz). Thermal properties, including the glass transition temperature (T_g), were determined by means of differential scanning calorimetry (DSC; TA2010) and thermogravimetric analysis (TGA; TA-2050) at a heating rate of 10 °C/min under nitrogen. Melting point (mp) was determined by means of DSC. Elemental analyses were performed by the National Center for Inter-University Research Facilities, Seoul National University (Elemental analyzer; CE Instruments Flash EA 1110). Absorption spectra were measured using a UV/vis spectrophotometer (K-MAC, Spectraview-2000). The molecular weight of the polymer was determined by gel permeation chromatography (GPC, Futecs, NS2001) using tetrahydrofuran (THF) as a solvent and calibrated against polystyrene standards. PL and EL spectra were obtained using a CCD

detecter (Princeton Instruments, SPEC-10) with a monochromator (Acton Research Co. SpectraPro-300i), and excitation sources were a xenon lamp with monochromator (Acton Research Co. SpectraPro-150) and Keithley 237 Source Measurement Unit, respectively. PLQEs were measured using the same detection system as PL, He−Cd laser (series 56, OmNichrome) as excitation source, and integrating sphere (Labsphere) for the collection of light. The current−voltage−luminescence characteristics of the devices were measured by using a Keithley 237 Source Measurement Unit and an optical power meter (Newport, 1835C) with a calibrated photodiode (Newport, 818 UV).

Electrochemical Analysis. CV measurements were conducted in a 0.1 M Bu_4NClO_4 solution in acetonitrile using a potentiostat (Eco Chemie, AUTOLAB) at a scan rate of 100 mV/s at room temperature. An ITO glass, a silver wire, and a platinum wire were used as the working electrode, reference electrode, and counter electrode, respectively. The reference electrode was calibrated using ferrocene. The half-wave potential for the oxidation of ferrocene was calculated as 4.80 eV from the vacuum energy level. Working electrodes were prepared by spin-coating using 10 mg/mL polymer solutions in chlorobenzene.

OLED Fabrication and Characterization. ITO glasses were cleaned using a washer (Mucasol, Merz) solution in an ultrasonic bath followed by acetone and methanol cleaning. Surface treatment was carried out by exposing the ITO glasses to UV-ozone. The hole injecting layer, PEDOT:PSS (Baytron-P 4083, Bayer), was spin-coated on the ITO glass with the thickness of 40 nm. The films were baked at 130 °C for 1 h in air. The films were baked under nitrogen again for 10 min. 15 mg/mL of PSAF polymer solutions was spin-coated on the PEDOT:PSS layer with the thickness of 70 nm and baked under nitrogen for 1 h. 5 nm of LiF, 20 nm of Ca, and 200 nm of Al layer were deposited by thermal evaporation method under 1×10^{-6} Torr. The active area of a device was 1 mm^2.

Material Synthesis. 10*H*-Spiro[anthracene-9,9′-(2′,7′-dibromofluorene)] was synthesized using the same way as our previous report.[33] Other starting materials were purchased from Aldrich Chemical Co. and used without further purification except THF, which was dried by refluxing over calcium hydride.

Tris(4-*tert*-butylphenyl)amine (1). A mixture of triphenylamine (2.45 g, 10 mmol), 2-methylpropan-2-ol (10 mL), and trifluoroacetic acid (40 mL) was stirred at room temperature for 5 days. During this period, precipitates appeared. The precipitate was filtered. It was redissolved in dichloromethane and recrystallized by addition of hexane. The product was white powder with 71% yield. ^{1}H NMR (300 MHz, $CDCl_3$): δ 1.30 (s, 27H), 7.01 (d, J = 8.3 Hz, 6H), 7.23 (d, J = 8.3 Hz, 6H). ^{13}C NMR (100 MHz, $CDCl_3$): δ 31.37, 34.14, 123.42, 125.93, 145.09, 145.44. Anal. Calcd for $C_{30}H_{38}N$: C, 87.11; H, 9.50; N, 3.39 Found: C, 87.00; H, 9.72; N, 2.98.

4-*tert*-Butyl-*N*,*N*-bis(4-*tert*-butylphenyl)-2-bromobenzenamine (2). 1 (4.13 g, 10 mmol) was dissolved in 150 mL of dichloromethane, and *N*-bromosuccinimide (NBS) (1.87 g, 10.5 mmol) in 50 mL of *N*,*N*-dimethylformamide (DMF) was added slowly using a dropping funnel under nitrogen. The solution was stirred at room temperature for 5 h and extracted by dichloromethane. The organic layer was dried over $MgSO_4$, and the solvents were evaporated. The crude product was recrystallized from dichloromethane and hexane. The product was a yellowish white powder with 85% yield. ^{1}H NMR (300 MHz, $CDCl_3$): δ 1.29 (s, 18H), 1.32 (s, 9H), 6.90 (d, J = 6.8 Hz, 4H), 7.22 (m, 5H), 7.31 (dd, J = 8.3, 2.4 Hz, 1H), 7.61 (d, J = 2.4 Hz, 1H). ^{13}C NMR (100 MHz, $CDCl_3$): δ 31.19, 31.37, 34.07, 34.51, 121.11, 123.73, 125.76, 125.99, 131.11, 131.34, 142.87, 144.29, 144.29, 144.62, 150.73. Anal. Calcd for $C_{30}H_{37}BrN$: C, 73.16; H, 7.78; N, 2.84 Found: C, 72.73; H, 7.80; N, 2.43.

2′,7′-Dibromo-10-(4-*tert*-butylphenyl)-2,7-di-*tert*-butyl-10*H*-spiro(ancridine-9,9′-fluorene) (3). Mg (0.31 g, 13 mmol) was charged into a two-neck flask and flame-dried. **2** (3.94 g, 8 mmol), in 10 mL of THF, was added to the flask. The reaction mixture was refluxed for 1 h under nitrogen and cooled to room temperature. 2,7-Dibromofluorenone (2.46 g, 7 mmol) was rapidly added to the reaction mixture, which was then refluxed for 2 h. After cooling the reaction mixture, the mixture was neutralized by the addition of 0.1 M HCl and extracted by ether. The organic layer was dried over $MgSO_4$ and evaporated. Unreacted starting materials were removed using short liquid column chromatography; the remainder was charged into a two-neck flask, and 100 mL of acetic acid and 1 mL of concentrated HCl solution were added. The mixture was refluxed for 6 h, and a white precipitate appeared during this period. The mixture was cooled to room temperature, and the precipitates were filtered and dried in a vacuum oven. The product was recrystallized twice from hot dichloromethane and methanol. The product was a white powder, in 69% yield. ^{1}H NMR (300 MHz, $CDCl_3$): δ 0.99 (s, 18H), 1.44 (s, 9H), 6.35 (m, 4H), 7.00 (dd, J = 8.6 Hz, 2.4 Hz, 2H), 7.36 (d, J = 8.2 Hz, 2H), 7.50 (dd, J = 8.1 Hz, 1.8, 2H), 7.55 (d, J = 1.8 Hz, 2H), 7.63 (d, J = 8.0 Hz), 2H), 7.68 (d, J = 8.4 Hz, 2H). ^{13}C NMR (100 MHz, $CDCl_3$): δ 31.05, 31.42, 33.73, 34.79, 53.37, 57.61, 114.38, 121.26, 122.08, 122.72, 124.09, 124.60, 127.86, 129.26, 130.41, 130.90, 137.24, 138.17, 139.45, 143.01, 151.51, 158.06. Anal. Calcd for $C_{43}H_{43}Br_2N$: C, 70.40; H, 5.91; N, 1.91 Found: C, 70.79; H, 5.91; N, 1.58.

10,10-Bis(hexadecyl)-10*H*-spiro[anthracene-9,9′-(2′,7′-dibromofluorene)] (4). 10*H*-Spiro[anthracene-9,9′-(2′,7′-dibromofluorene)] (4.88 g, 10 mmol), an excess of KH, a catalytic amount of 18-crown-6, and 10 mL of THF were placed in a two-neck flask. 1-Bromohexadecane (12.2 g, 40 mmol) was injected, and the solution was stirred for 5 h at room temperature. The remaining KH was deactivated by slow addition of methanol. The reaction mixture was extracted with 300 mL of ether. The solution was dried over $MgSO_4$ and evaporated. The reaction mixture was purified by column chromatography using hexane:dichloromethane (0.99:0.1, R_f = 0.45). The product was a white powder, in 69% yield. ^{1}H NMR (300 MHz, $CDCl_3$, ppm): δ 0.87 (m, 10), 1.24 (m, 52), 2.16 (m, 4H), 6.24 (dd, J = 7.9 Hz, 1.3 Hz, 2H), 6.89 (td, J = 6.9 Hz, 1.1 Hz, 2H), 7.07 (d, J = 1.6 Hz, 2H), 7.23 (m, 2H), 7.46 (m, 4H), 7.63 (d, 8.3 Hz, 2H). ^{13}C NMR (100 MHz, $CDCl_3$, ppm): δ 14.04, 22.60, 25.74, 29.27, 29.40, 29.50, 29.51, 29.57, 29.60, 30.03, 31.85, 45.66, 46.72, 57.88, 76.58, 121.26, 122.41, 126.02, 126.27, 127.54, 128.61, 129.15, 130.70, 136.34, 138.25, 139.31, 160.02. Anal. Calcd for $C_{58}H_{80}Br_2$: C, 74.34; H, 8.61. Found: C, 75.17; H, 8.91.

Polymer Synthesis. 0.69 g of bis(2,5-cyclooctadiene)nickel(0), 0.39 g of dipyridyl, and 0.30 mL of 1,5-cyclooctadiene were placed on a two-neck flask. 15 mL of anhydrous DMF was injected, and the solution was then stirred at 80 °C for about 30 min. When the color of the solution became dark-blue, 1 mmol of mixture of monomers (**3**:**4** = 7:3, 5:5, 3:7, 1:9, 0:10) in 60 mL of toluene was injected to the solution. The solution was stirred at 80 °C for 24 h. The reaction mixture was poured into the mixture of 250 mL of methanol and concentrated HCl (methanol:HCl = 8:2), and the resulting precipitate was collected. The precipitate was redissolved in chloroform and reprecipitated using methanol several times. PSAF16 and PSAF-T1 were pale yellow powders, and the other polymers were white powders. The yields of polymers were from 40 to 65%. **PSAF16.** ^{1}H NMR (300 MHz, $CDCl_3$, ppm): δ 0.83 (m, 6H), 1.16 (m, 56H), 2.18 (br, 4H), 6.24 (m, 2H), 6.74 (m, 2H), 7.14 (m, 6H), 7.43 (br, 4H). Anal. Calcd for $C_{58}H_{80}$: C, 89.63; H, 10.37. Found: C, 90.41; H, 10.85. **PSAF-T1** (copolymer from 90 mol % SAF in the feed): C, 88.99; H, 10.29. **PSAF-T3** (copolymer from 70 mol % SAF in the feed): C, 90.27; H, 10.07; N, 0.16. **PSAF-T5** (copolymer from 50 mol % SAF in the feed): C, 90.09; H, 9.54; N, 0.70. **PSAF-T7** (copolymer from 30 mol % SAF in the feed): C, 89.30; H, 8.74; N, 0.58.

Acknowledgment. We thank the Ministry of Science and Technology, BK21 program, and National Research Laboratory program of KOSEF for financial support.

References and Notes

(1) Sheats, J. R.; Antoniadis, H.; Hueschen, M.; Leonard, W.; Miller, J.; Moon, R.; Roitman, D. B.; Stocking, A. *Science* **1996**, *273*, 884.
(2) Friend, R. H.; Gymer, R. W.; Holmes, A. B.; Burroughes, J. H.; Bradley, D. D. C.; Dos Santos, D. A.; Bredas, J. L.; Loglund, M.; Salaneck, W. R. *Nature (London)* **1999**, *397*, 121.

(3) Bernius, M. T.; Inbasekaran, M.; O'Brien, J.; Wu, W. *Adv. Mater.* **2000**, *12*, 1737.
(4) Forrest, S. R. *Nature (London)* **2004**, *428*, 911.
(5) Kim, D. Y.; Cho, H. N.; Kim, C. Y. *Prog. Polym. Sci.* **2000**, *25*, 1089.
(6) Sherf, U. *J. Mater. Chem.* **1999**, *9*, 1853.
(7) Kreyenschmidt, M.; Klaerner, G.; Fuhrer, T.; Ashenhurst, J.; Karg, S.; Chen, W. D. Lee, V. Y.; Scott, J. C.; Miller, R. D. *Macromolecules* **1998**, *31*, 1099.
(8) Sherf, U.; List, E. J. W. *Adv. Mater.* **2002**, *14*, 477.
(9) Leclerc, M. *J. Polym. Sci., Part A: Polym. Chem.* **2001**, *39*, 2867.
(10) List, E. J. W.; Guentner, R.; Scanducci de Freitas, P.; Sherf, U. *Adv. Mater.* **2002**, *14*, 374.
(11) Weinfurtner, K. H.; Fujikawa, H.; Tokito, S.; Taga, Y. *Appl. Phys. Lett.* **2000**, *76*, 2502.
(12) Grell, M.; Bradley, D. D. C.; Ungar, G.; Hill, J.; Whitehead, K. S. *Macromolecules* **1999**, *32*, 5810.
(13) Xia, C.; Advincula, R. C. *Macromolecules* **2001**, *34*, 5854.
(14) Zeng, G.; Yu, W. L.; Chua, S. J.; Huang, W. *Macromolecules* **2002**, *35*, 6907.
(15) Cheun, H.; Tanto, B.; Chunwaschirasiri, W.; Larson, B.; Winokur, M. J. *Appl. Phys. Lett.* **2004**, *84*, 22.
(16) Gong, X.; Iyer, P. K.; Moses, D.; Bazan, G. C.; Heeger, A. J.; Xiao, S. S. *Adv. Funct. Mater.* **2003**, *13*, 325.
(17) Gamerith, S.; Nothofer, H.-G.; Scherf, U.; List, E. J. W. *Jpn. J. Appl. Phys.* **2004**, *43*, L891.
(18) Kulkarni, A. P.; Kong, X.; Jenekhe, S. A. *J. Chem. B.* **2004**, *108*, 8689.
(19) Gong, X.; Moses, D.; Heeger, A. J.; Xiao, S. *Synth. Met.* **2004**, *141*, 17.
(20) Klärner, G.; Lee, J.-I.; Lee, V. Y.; Chan, E.; Chen, J.-P.; Nelson, A.; Markiewicz, D.; Siemens, R.; Scott, J. C.; Miller, R. D. *Chem. Mater.* **1999**, *11*, 1800.
(21) Marsitzky, D.; Murray, J.; Scott, J. C.; Carter, J. R. *Chem. Mater.* **2001**, *13*, 4285.
(22) Klärner, G.; Davey, M. H.; Chen, W.-D.; Scott, J. C.; Miller, R. D. *Adv. Mater.* **1998**, *10*, 993.
(23) Kulkarni, A. P.; Jenekhe, S. A. *Macromolecules* **2003**, *36*, 5285.
(24) Xia, Chuanjun; Advincula, R. C. *Macromolecules* **2001**, *34*, 5854.
(25) Byun, H. Y.; Chung, I. J.; Shim, H.-K.; Kim, C. Y. *Chem. Phys. Lett.* **2004**, *393*, 197.
(26) Pei, J.; Liu, X.-L.; Chen, Z.-K.; Zhang, X.-H.; Lai, Y.-H.; Huang, W. *Macromolecules* **2003**, *36*, 323.
(27) Setayesh, S.; Grimsdale, A. C.; Weil, T.; Enkelmann, V.; Müllen, K.; Meghdadi, F.; List, E. J. W.; Leising, G. *J. Am. Chem. Soc.* **2001**, *123*, 946.
(28) Pogantsch, A.; Wenzl, F. P.; List, E. J. W.; Leising, G.; Grimsdale, A. C.; Müllen, K. *Adv. Mater.* **2002**, *14*, 1061.
(29) Lupton, J. M.; Schouwink, P.; Keivanidis, P. E.; Grimsdale, A. C.; Müllen, K. *Adv. Funct. Mater.* **2003**, *13*, 154.
(30) Marsitzky, D.; Vestberg, R.; Blainey, P.; Tang, B. T.; Hawker, C. J.; Carter, K. R. *J. Am. Chem. Soc.* **2001**, *123*, 6965.
(31) Jacob, J.; Zhang, J.; Grimsdale, A. C.; Müllen, K.; Gaal, M.; List, E. J. W. *Macromolecules* **2003**, *36*, 8240.
(32) Yu, W.-L.; Pei, J.; Huang, W.; Heeger, A. J. *Adv. Mater.* **2000**, *12*, 828.
(33) Vak, D.; Chun, C.; Lee, C. L.; Kim, J.-J.; Kim, D.-Y. *J. Mater. Chem.* **2004**, *14*, 1342.
(34) Vak, D.; Lim, B.; Lee, S.-H.; Kim, D.-Y. *Org. Lett.* **2005**, *7*, 4229.
(35) Tseng, Y.-H.; Shih, P.-I.; Chien, C.-H.; Dixit, A. K.; Shu, C. F.; Liu, Y. H.; Lee, G.-H. *Macromolecules* **2005**, *38*, 10055.
(36) Xia, R.; Heliotis, G.; Campoy-Quiles, M.; Stavrinou, P. N.; Bradley, D. D. C.; Vak, D.; Kim, D.-Y. *J. Appl. Phys.* **2005**, *98*, 083101.
(37) Neher, D. *Macromol. Rapid Commun.* **2001**, *22*, 1365.
(38) Brown, T. M.; Kim, J. S.; Friend, R. H.; Cacialli, F.; Daik, R.; Feast, W. J. *Appl. Phys. Lett.* **1999**, *75*, 1679.
(39) Ego, C.; Grimsdale, A. C.; Uckert, F.; Yu, Gang; Srdanov, G.; Müllen, K. *Adv. Mater.* **2002**, *14*, 809.
(40) Shu, C.-F.; Dodda, R.; Wu, F.-I.; Liu, M. S.; Jen, A. K.-Y. *Macromolecules* **2003**, *36*, 6698.
(41) Miteva, T.; Meisel, A.; Knoll, W.; Nothofer, H. G.; Scherf, U.; Müller, D. C.; Meerholz, K.; Yasuda, A.; Neher, D. *Adv. Mater.* **2001**, *13*, 565.
(42) Vak, D.; Shin, S. J.; Yum, J.-H.; Kim, S.-S.; Kim, D.-Y. *J. Lumin.* **2005,** *115*, 109.
(43) Mitchell, R. H.; Lai, Y.-H.; Williams, R. V. *J. Org. Chem.* **1979**, *44*, 4733.
(44) Teetsov, J.; Fox, M. A. *J. Mater. Chem.* **1999**, *9*, 2117.
(45) de Mello, J. C.; Felix Wittmann, H.; Friend, R. H. *Adv. Mater.* **1997**, *9*, 230.
(46) Greenham, N. C.; Samuel, I. D. W.; Hayes, G. R.; Phillips, R. T.; Kessener, Y. A. R. R.; Moratti, S. C.; Holmes, A. B.; Friend, R. H. *Chem. Phys. Lett.* **1995**, *241*, 89.
(47) Cho, H.-J.; Jung, B.-J.; Cho, N. S.; Lee, J.; Shim, H.-K. *Macromolecules* **2003**, *36*, 6704.
(48) Brown, T. M.; Friend, R. H.; Millard, I. S.; Lacey, D. J.; Burroughes, J. H.; Cacialli, F. *Appl. Phys. Lett.* **2001**, *79*, 174.

MA060683O